Identification of a hydrogen bond in the Phe M197→Tyr mutant reaction center of the photosynthetic purple bacterium *Rhodobacter sphaeroides* by X-ray crystallography and FTIR spectroscopy[1]

Andreas Kuglstatter[a,2], Petra Hellwig[b], Günter Fritzsch[a,*], Josef Wachtveitl[c,3], Dieter Oesterhelt[c], Werner Mäntele[b], Hartmut Michel[a]

[a] *Max-Planck-Institut für Biophysik, Heinrich-Hoffmann-Str. 7, D-60528 Frankfurt/M., Germany*
[b] *Institut für Biophysik, J.W. Goethe-Universität, Theodor-Stern-Kai 7, Haus 74, D-60590 Frankfurt/M., Germany*
[c] *Max-Planck-Institut für Biochemie, Am Klopferspitz 18a, D-82152 Martinsried, Germany*

Received 20 October 1999; received in revised form 10 November 1999

Edited by Richard Cogdell

Abstract In bacterial reaction centers the charge separation process across the photosynthetic membrane is predominantly driven by the excited state of the bacteriochlorophyll dimer (D). An X-ray structure analysis of the Phe M197→Tyr mutant reaction center from *Rhodobacter sphaeroides* at 2.7 Å resolution suggests the formation of a hydrogen bond as postulated by Wachtveitl et al. [Biochemistry 32, 12875–12886, 1993] between the Tyr M197 hydroxy group and one of the 2a-acetyl carbonyls of D. In combination with electrochemically induced FTIR difference spectra showing a split band of the π-conjugated 9-keto carbonyl of D, there is clear evidence for the existence of such a hydrogen bond.

Key words: Photosynthetic reaction center; Primary donor; Site-directed mutagenesis; X-ray crystallography; Fourier transform infrared spectroscopy

1. Introduction

The photosynthetic reaction center (RC) of the purple bacterium *Rhodobacter (Rb.) sphaeroides* is a membrane-spanning protein–pigment complex that converts light energy to chemical free energy. The three-dimensional structure of the RC has been determined with increasing resolution [1–3]. The RC core consists of two protein subunits (L and M) showing a quasi-C_2 symmetry with its twofold axis perpendicular to the photosynthetic membrane. In the same symmetrical manner, L and M bind a bacteriochlorophyll *a* dimer (D), two monomeric bacteriochlorophylls *a*, two bacteriopheophytins *a*, two ubiquinones-10, and one non-heme iron. Two branches of cofactors (A and B) are formed from D, which is located near the periplasmic RC surface, to the ubiquinones, which are bound close to the cytoplasmic protein boundary. Each branch consists of one D-associated bacteriochlorophyll (D_A and D_B, respectively), a monomeric bacteriochlorophyll, a bacteriopheophytin, and a quinone molecule.

The charge separation process in bacterial RCs at physiological conditions is predominantly driven by the excited state of D that acts as the primary electron donor (reviewed in [4,5]). Resonance energy transfer from light-harvesting complexes to the RC or light absorption by the RC itself results in the electronic excitation D→D*. Despite the symmetrical cofactor arrangement in the RC protein, an electron is transferred unidirectionally along branch A from D* to the A-sided ubiquinone. Attempts to change this unidirectionality of electron transfer by site-directed mutagenesis of amino acid residues situated along branch A had no success [6–8], until recently M-sided electron transfer in mutant RCs was reported [9,10]. Quantum chemical calculations suggest that differences in the distances between the electron transfer cofactors of the two branches are responsible for the unidirectionality of electron transfer, whereas protein effects on the unidirectionality are assumed to be small [11]. Although the apoprotein shows an approximate C_2 symmetry, characteristic deviations are observed at the level of individual amino acids [2,12] leading to an asymmetric charge distribution of the cation radical state of D ($D^{+\bullet}$) [13–15].

The Phe M197→Tyr (M197FY) mutant RC of *Rb. sphaeroides* has been constructed in order to study the effects of hydrogen bonding on the physical properties of D [16]. In the homologous structure of the *Rhodopseudomonas (Rp.) viridis* RC, the corresponding Tyr M195 (in the following, this residue is called Tyr M197 according to its sequence position in the *Rb. sphaeroides* RC) forms a hydrogen bond to the π-conjugated 2a-acetyl carbonyl of D_B [17]. Therefore, the M197FY mutant RC of *Rb. sphaeroides* allows analysis of the effect of a non-conserved hydrogen bond between D and the apoprotein. Fourier transform Raman (FT-Raman) spectra of the M197FY RC show a band shift from 1653 cm^{-1} in the native RC to 1636 cm^{-1} in the mutant protein [16]. The band at 1653 cm^{-1} in the wild-type RC has been assigned to the stretching frequency of a free 2a-acetyl carbonyl of D [14]. Consequently, the band shift of 17 cm^{-1} to lower vibrational energy has been interpreted in terms of a hydrogen-bonded 2a-acetyl carbonyl of D_B [16]. No band assignment was pos-

*Corresponding author. Fax: (49)-69-96769 423.
E-mail: fritzsch@mpibp-frankfurt.mpg.de

[1] Parts of the crystallographic results presented in this article have already been published in G. Garab (Ed.) (1998) Photosynthesis: Mechanisms and Effects, Vol. II, pp. 699–702, Kluwer Academic, Dordrecht.

[2] Present address: MRC Laboratory of Molecular Biology, Hills Road, Cambridge CB2 2HQ, UK.
[3] Present address: Institut für Medizinische Optik, Ludwig-Maximilians-Universität, Oettingenstr. 67, D-80538 Munich, Germany.

Abbreviations: D, bacteriochlorophyll dimer; FTIR, Fourier transform infrared; FT-Raman, Fourier transform Raman; M197FY, Phe M197→Tyr; RC, reaction center

0014-5793/99/$20.00
PII: S0014-5793(99)01614-2

sible using light-induced Fourier transform infrared (FTIR) difference spectroscopy [18]. To obtain information about the hydrogen bonding geometry and possible structural changes in the protein environment we have determined the structure of the M197FY mutant RC by X-ray diffraction analysis. In addition, electrochemically induced FTIR difference spectra have been recorded to complete the structure-based discussion of the mutant RC.

2. Materials and methods

M197FY mutant RCs [16] and wild-type RCs were purified using centrifugation and anion exchange chromatography as reviewed in [19].

2.1. X-ray crystallography

The RCs were crystallized in detergent micelles (*N*,*N*-dimethyldodecylamine-*N*-oxide) applying the vapor diffusion method with potassium phosphate as precipitant [20]. Three-dimensional RC crystals of space group $P3_121$ with unit cell dimensions $a = b = 142$ Å, $c = 187$ Å and a maximum size of $2.0 \times 1.0 \times 1.0$ mm^3 grew after about 2 weeks. X-ray diffraction data were collected on a 345 mm MAR-Research imaging plate detector at the MPG-ASMB-BW6 synchrotron beamline (DORIS-ring/DESY, Hamburg). Data processing was performed using the program package HKL [21]. The software package CNS [22] was used for crystallographic model refinement. The refinement was achieved using rigid-body refinement of the wild-type model [2] against the mutant data, overall temperature-factor refinement, bulk solvent correction, simulated annealing, conjugate gradient minimization, and individual temperature-factor refinement. To determine the position of the introduced Tyr M197 side chain and its surroundings without model bias, a simulated annealing omit map [23] was calculated omitting all atoms within 8 Å of the exchanged amino acid and applying harmonic restraints to atoms within a 2 Å cushion. Geometric parameters of Engh and Huber [24] for the polypeptide chain and parameters of Treutlein et al. [25], Lancaster and Michel [26], and U. Ermler (unpublished data) for the cofactors were applied in the crystallographic refinement. Manual rebuilding of the structure model was performed with the graphics program O [27], and the structure figures were produced with the graphics program SETOR [28].

2.2. FTIR spectroscopy

For FTIR measurements, the B-sided ubiquinone was exchanged against the electron transfer inhibitor terbutryn [29]. The RCs were transferred to D_2O phosphate buffer with *n*-octyl-β-D-glucopyranoside as detergent and concentrated up to 1.0 mM [30]. Within the limits of resolution, the VIS/NIR spectrum of the final RC sample is identical to the spectrum of the RC solution before the removal of the B-sided quinone (data not shown). The ultra-thin-layer electrochemical cell was used as described previously [31,32], for mediator and modifier see [33,34], respectively. All potentials are quoted vs. the Ag/AgCl/3 M KCl reference electrode. For values vs. standard hydrogen electrode (pH 7.0) add 208 mV. The potentials are accurate within about 5 mV. FTIR spectra were recorded on a modified Bruker IFS25 FTIR spectrometer. For each spectrum 128 interferograms are averaged using triangular apodization. To improve signal to noise ratios five spectra were added. Absorbance spectra in the VIS/NIR spectral region were measured simultaneously to the IR as described in [35]. Spectra were recorded with 4 cm^{-1} spectral resolution in the IR and 1 nm resolution in the VIS/NIR region.

Table 1
Data collection and refinement statistics

Data[a]	
Resolution	2.7 Å
Number of unique reflections	52 235
Completeness	87.2% (90.6%)
Multiplicity	2.2 (2.1)
R_{sym}^{b}	7.1% (31.0%)
Refinement	
R_{free}^{c}	21.7%
R_{cryst}	18.8%
Mean coordinate error[d]	0.37 Å
R.m.s.d.[e]	
bond length	0.007 Å
bond angles	1.1°
Residues in Ramachandran plot [38]	
most favored areas	91.8%
additional favored areas	7.8%
generously allowed areas	0.4%
disallowed areas	0.0%

[a]Figures in parentheses refer to the statistics for the outer resolution shell (2.8–2.7 Å).
[b]*R* factor on symmetry-related intensities.
[c]Cross-validated *R* factor [36].
[d]R_{free}-based estimate of the mean coordinate error from a Luzzati plot [37].
[e]Root mean square deviations from ideal geometry values as mentioned in Section 2.1.

3. Results

3.1. X-ray structure determination of the M197FY mutant RC

The data collection and refinement statistics are listed in Table 1. 52 235 unique reflections were measured up to 2.7 Å resolution yielding a completeness of 87.2% and a multiplicity of 2.2. The R_{sym} factor of the intensities of symmetry-

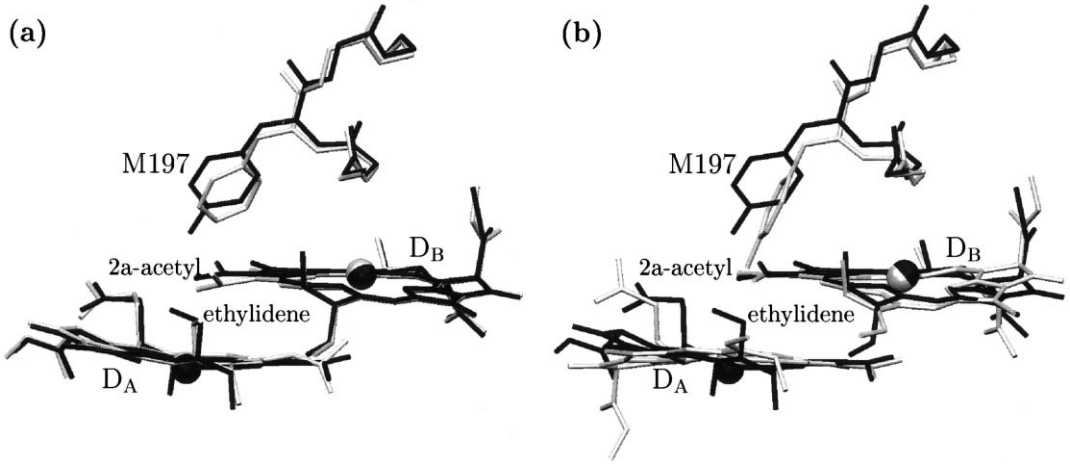

Fig. 1. a: *Rb. sphaeroides* M197FY RC (dark) and wild-type RC (light). b: *Rb. sphaeroides* M197FY RC (dark) and *Rp. viridis* wild-type RC (light). The structures have been superimposed by applying a least square minimization to the coordinates of all C^{α} atoms and tetrapyrrole nitrogens within 20 Å of the site of amino acid exchange.

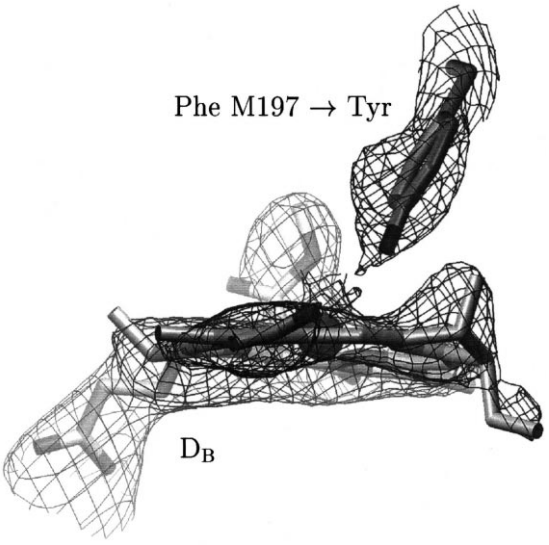

Fig. 2. $2|F_{obs}|-|F_{calc}|$ simulated annealing omit map of the M197FY RC contoured at 1.8 S.D. above the mean electron density. View along the D_B 2a-acetyl axis.

related reflections is 7.1%. The refinement process converged at a free R factor [36] of 21.7% and a conventional crystallographic R factor of 18.8%. The R_{free}-based estimate of the average coordinate error is 0.37 Å as derived from a Luzzati plot [37]. The low deviations of the mutant RC model from ideal stereochemistry and the Ramachandran statistics [38] underline the high quality of the structure model.

The structures of the wild-type RC [2] (PDB [39] entry code 1PCR) and the M197FY mutant RC are superimposed in Fig. 1a. The introduced Tyr M197 shows the same orientation within the protein as the native Phe. A simulated annealing omit map shows the position of the D_B 2a-acetyl group (Fig. 2), but its orientation remains undetermined concerning a 180° rotation around the acetyl $>C–C(D_B)$ axis, since acetyl carbonyl and methyl groups cannot be distinguished in electron density maps at the present resolution. In the structure presented here, the 2a-acetyl oxygen points towards Tyr M197 (see Section 4). The distance between the hydroxy oxygen of Tyr M197 and the acetyl oxygen of D_B is 2.6 Å. The angle formed by (1) the Tyr carbon atom next to the hydroxy oxygen, (2) the Tyr hydroxy oxygen itself, and (3) the D_B acetyl oxygen is 117°. In the mutant RC the peptide backbone at position M197 is shifted up to 0.5 Å away from D as compared to the native protein. (The root mean square deviation between the C^{α} atoms in the wild-type and mutant RC structures is 0.3 Å.) No further structural changes are observed at the present resolution either in D_B or in the protein environment.

3.2. Electrochemically induced FTIR difference spectroscopy

The electrochemically induced FTIR difference spectra of the wild-type RC and of the M197FY mutant RC equilibrated in D_2O are superimposed in Fig. 3. The most prominent feature of the M197FY mutant spectrum is an additional band at 1716 cm^{-1} compared to a weak shoulder in the wild-type

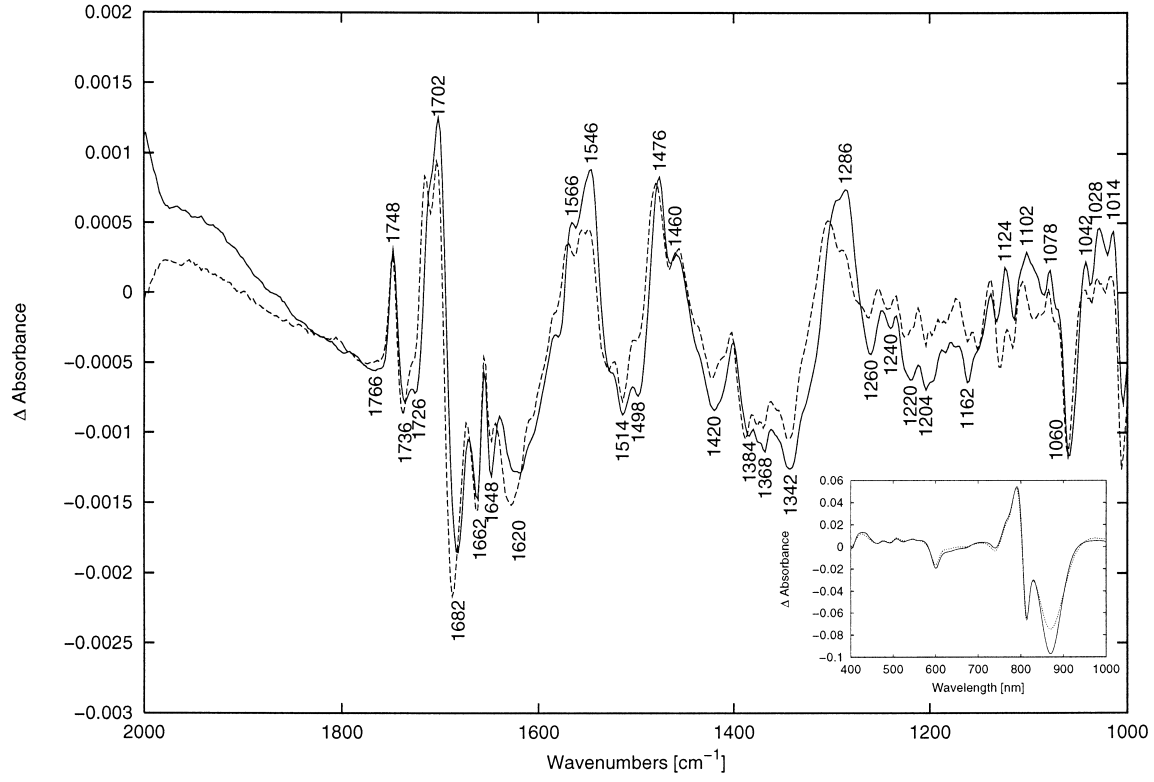

Fig. 3. Electrochemically induced FTIR difference spectra (+0.4 minus 0 V) of wild-type (solid line) and M197FY mutant RC (dashed line) equilibrated in D_2O. Inset: the corresponding VIS/NIR difference spectra. Positive bands correlate with the oxidized state of the protein and negative bands with the reduced state. To superimpose the difference spectra, the bands are normalized according to the VIS/NIR bands at 791 nm and 814 nm. Only frequencies for the wild-type RC are labelled.

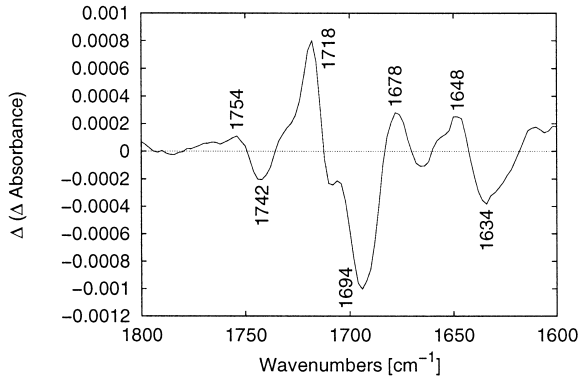

Fig. 4. M197FY-minus-native double difference spectrum of RCs equilibrated in D_2O. The corresponding difference spectra are shown in Fig. 3.

spectrum. The minima in the spectrum of the native RC at 1682 cm^{-1} and 1620 cm^{-1} are shifted in the mutant protein to 1688 cm^{-1} and 1628 cm^{-1}, respectively. Another difference between wild-type and mutant spectra is observed in the region around 1290 cm^{-1}. Maxima at 1286 cm^{-1} and 1294 cm^{-1} in the native difference spectrum correlate with bands at 1290 cm^{-1} and 1304 cm^{-1} in the M197FY mutant spectrum. Further band shifts occur at 1130 cm^{-1} and in the 1460–1480 cm^{-1} region. Except for the region of water absorption (1650 ± 30 cm^{-1}), no significant shifts are observed after H/D exchange (spectrum of RCs equilibrated in H_2O are not shown here).

The inset in Fig. 3 shows electrochemically induced VIS/NIR difference spectra. The most prominent feature of the mutant spectrum is the reduction of the band amplitude at 870 nm. This observation correlates with light-induced difference spectra as reported in [16].

4. Discussion

4.1. X-ray structure of the M197FY mutant RC

In contrast to the structure of the Phe M197→Arg/Tyr M177→Phe double mutant RC, in which the introduced Arg M197 side chain points towards the opposite direction compared to the native Phe M197 [40], Tyr M197 in the M197FY mutant RC shows an orientation like Phe M197 in the native protein (Fig. 1a). The arrangement of the Tyr M197 hydroxy group as putative proton donor and the π-conjugated 2a-acetyl carbonyl of D_B as putative proton acceptor allows hydrogen bonding according to hydrogen bonding statistics [41,42]. However, electron density maps at 2.7 Å resolution do not allow a distinction to be made between the carbonyl oxygen and the methyl carbon. Therefore, the structure of the 2a-acetyl carbonyl remains undetermined concerning a 180° rotation around its acetyl $>$C–C(D_B) axis. Consequently, X-ray structure analysis of the M197FY mutant RC highly suggests hydrogen bonding, but it does not provide enough information to prove the existence of the bond. This is possible only in combination with spectroscopic measurements (see Section 4.2).

The 0.5 Å shift at position M197 in the structural model of the M197FY mutant RC (Fig. 1a) compared to the wild-type structure results from the crystallographic refinement process, but it is not backed by difference electron density calculations at the present resolution (2.7 Å). However, this shift is plausible for structural reasons. The theoretical substitution of Phe M197 by Tyr in the wild-type RC without any further structural changes would lead to a distance of 2.3 Å between the introduced hydroxy oxygen and the D_A ethylidene group, which implies overlapping of van der Waals spheres. Therefore, it can be envisaged that the Tyr M197 phenyl ring in the mutant RC structure would take up a position further away from the ethylidene group than the corresponding ring in the native RC (Fig. 1a). This ethylidene group of D_A in the *Rb. sphaeroides* RC is not in the porphyrin plane. In the homologous RC of the purple bacterium *Rp. viridis* the same ethylidene group has an in-plane configuration ([17], PDB entry code 1PRC), explaining why Tyr M197 in the native *Rp. viridis* RC is located closer to D compared to the mutated Tyr M197 in the *Rb. sphaeroides* protein (Fig. 1b).

The mutation M197FY in the *Rb. sphaeroides* RC brings the only non-conserved amino acid in this part of the protein into line with the sequence of the *Rp. viridis* RC. Therefore, large structural changes between the RCs of both species are not expected. However, the Tyr M197 phenyl rings in the *Rb. sphaeroides* mutant RC and the *Rp. viridis* wild-type RC are oriented almost perpendicular to each other (Fig. 1b). This difference might result from unresolved structural differences between both RCs.

In the Phe M197→His mutant RC of *Rb. sphaeroides* the formation of a hydrogen bond between the introduced His M197 and the D_B 2a-acetyl carbonyl results in an increase of the midpoint potential of D by 125 mV [43]. In the M197FY mutant RC studied here, the analogous hydrogen bond with the mutated Tyr M197 as proton donor causes an upshift of the D midpoint potential by 30 mV only [16]. In [44] it is suggested that the formation of a hydrogen bond between the 2a-acetyl carbonyl of D_B and His M197 might lead to a reorientation of the D_B acetyl carbonyl. This would explain the remarkable increase of the midpoint potential of D in the Phe M197→His mutant RC as postulated in [43,45]. For the M197FY RC no significant reorientation of the 2a-acetyl carbonyl is observed at the present resolution (Fig. 2), correlating to the weak increase in the D midpoint potential of the M197FY protein.

The structural similarity of the native and the M197FY mutant RCs except for the exchanged amino acid residue confirms a posteriori that the changed physical properties of D in the M197FY RC [16] are due to the generated hydrogen bond and are not influenced by additional structural changes that are detectable within the limits of resolution applicable to this study. A local rearrangement of the protein around the B-sided bacteriopheophytin as proposed in [46] is not observed in the mutant crystal structure within the limits of the present resolution.

4.2. Electrochemically induced FTIR difference spectra

The positive band at 1702 cm^{-1} in the $D^{+\bullet}$/D spectrum of the wild-type RC (Fig. 3) has been assigned to the stretching mode of free 9-keto C=O groups of D in its oxidized state [30]. The corresponding negative band of the reduced dimer appears in the spectrum of the native protein at 1682 cm^{-1}. This band is shifted to 1688 cm^{-1} in the M197FY mutant RC whereas the positive 9-keto band splits into two bands at 1704 cm^{-1} and 1716 cm^{-1} (Fig. 3), yielding the most prominent band shift in the M197FY-minus-native double difference

spectrum at 1694 cm^{-1}(−)/1718 cm^{-1}(+) (Fig. 4). Most likely, this change in the spectral properties of the RC results from the additional hydrogen bond between the introduced Tyr M197 and the 2a-acetyl carbonyl of D_B. In the bacteriochlorophyll *a* molecule a system of conjugated double bonds extends from the 2a-acetyl oxygen to the 9-keto oxygen at the opposite side of the porphyrin ring. This pronounced π-bonding system allows the detection of a perturbation at the 2a-acetyl oxygen by a changed stretching frequency of the 9-keto group. The wild-type band at 1702 cm^{-1} represents the superimposed stretching frequencies of the D_A and D_B 9-keto groups. The fact that in the mutant spectrum a band splitting rather than a simple band shift is observed indicates that only one of the two D keto groups is influenced by the mutation. Consequently, the band at 1716 cm^{-1} in the M197FY spectrum can be assigned to the 9-keto C=O stretching of D_B, whereas the unshifted 1702 cm^{-1} band belongs to the analogous stretching mode of D_A.

In contrast to the results obtained by electrochemically induced FTIR difference spectroscopy, no splitting of the 9-keto band has been observed when recording photochemically induced FTIR difference spectra [18]. Polarization artifacts caused by anisotropic drying of the RC sample in the case of the light-induced measurements cannot explain this inconsistency, since the 9-keto groups of D are oriented almost in parallel to each other. However, several prominent differences appear between electrochemically induced [30] and photochemically induced [18] FTIR difference spectra of the wild-type RC. These discrepancies could not be clarified yet.

In the native RC, the 2a-acetyl C=O stretching frequencies of D_A and D_B are expected between 1620 cm^{-1} and 1650 cm^{-1} [35]. The discussed hydrogen bond between Tyr M197 and the 2a-acetyl oxygen of D_B in the M197FY mutant RC is expected to lead to a band shift in this spectral region to lower stretching frequencies. A comparable shift has been observed recording FT-Raman spectra of this mutant RC [16]. However, an unambiguous assignment of the bands between 1620 cm^{-1} and 1665 cm^{-1} measured by FTIR difference spectroscopy is not possible, because of the strong amide I absorption and the superposition of several other group frequencies. The band shift from 1648 cm^{-1} to 1634 cm^{-1} in the M197FY-minus-native double difference spectrum (Fig. 4) is tentatively assigned to the shifted 2a acetyl C=O stretching frequency.

The band shifts to lower vibration frequencies at 1130 cm^{-1}, 1300 cm^{-1}, 1460 cm^{-1}, and 1480 cm^{-1} in the M197FY mutant spectrum may result from changed vibrations of the D_B tetrapyrrole ring, which are induced by the hydrogen bond not present in the native RC between D_B and the apoprotein. This assignment is supported by the observation that in both the wild-type and the mutant spectra the positions of the band maxima are the same for samples equilibrated in H_2O (data not shown) or D_2O. No groups with vibrational frequencies sensitive to H/D exchange should be involved in the spectral modifications caused by the mutation.

Both FT-Raman [16] and FTIR spectra suggest the formation of the supposed hydrogen bond in the M197FY mutant RC. Its X-ray structure supports this idea because the introduced Tyr M197 obeys hydrogen bonding geometry and because no further structural changes occur compared to the wild-type protein (Fig. 1a). Therefore, X-ray diffraction analysis in combination with FT-Raman or FTIR spectroscopic measurements shows unambiguously the existence of the hydrogen bond between the apoprotein and D_B in the M197FY mutant RC.

Acknowledgements: We thank Ulrich Ermler for helpful discussions, Zlata Bojadzijev and Gregor Eichberger for technical assistance, and Hans Bartunik (MPG-ASMB c/o DESY, Hamburg) for support at beamline BW6 (DORIS-ring, DESY).

References

[1] Allen, J.P., Feher, G., Yeates, T.O., Komiya, H. and Rees, D.C. (1988) Proc. Natl. Acad. Sci. USA 85, 8487–8491.
[2] Ermler, U., Fritzsch, G., Buchanan, S.K. and Michel, H. (1994) Structure 2, 925–936.
[3] Stowell, M.H.B., McPhillips, T.M., Rees, D.C., Soltis, S.M., Abresch, E. and Feher, G. (1997) Science 276, 812–816.
[4] Woodbury, N.W. and Allen, J.P. (1995) in: Anoxygenic Photosynthetic Bacteria (Blankenship, R.E., Madigan, M.T. and Bauer, C.E., Eds.), Advances in Photosynthesis, Vol. 2, pp. 527–557, Kluwer Academic, Dordrecht.
[5] van Brederode, M.E. and van Grondelle, R. (1999) FEBS Lett. 455, 1–7.
[6] Bylina, E.J., Kirmaier, C., McDowell, L., Holten, D. and Youvan, D.C. (1988) Nature 336, 182–184.
[7] Finkele, U., Lauterwasser, C., Zinth, W., Gray, K.A. and Oesterhelt, D. (1990) Biochemistry 29, 8517–8521.
[8] Nagarajan, V., Parson, W.W., Gaul, D. and Schenck, C. (1990) Proc. Natl. Acad. Sci. USA 72, 3491–3495.
[9] Kirmaier, C., Weems, D. and Holten, D. (1999) Biochemistry 38, 11516–11530.
[10] Heller, B.A., Holten, D. and Kirmaier, C. (1995) Science 269, 940–945.
[11] Hasegawa, J. and Nakatsuji, H. (1998) J. Phys. Chem. B 102, 10420–10430.
[12] Ermler, U., Michel, H. and Schiffer, M. (1994) J. Bioenerg. Biomembr. 26, 5–15.
[13] Lendzian, F., Enderward, B., Plato, M., Bumann, D., Lubitz, W. and Möbius, K. (1990) in: Reaction Centers of Photosynthetic Bacteria (Michel-Beyerle, M.-E., Ed.), Springer Series in Biophysics, Vol. 6, pp. 57–68, Springer-Verlag, Berlin.
[14] Mattioli, T.A., Hoffmann, A., Robert, B., Schrader, B. and Lutz, M. (1991) Biochemistry 30, 4648–4654.
[15] Rautter, J., Geßner, C., Lendzian, F., Lubitz, W., Williams, J.C., Murchison, H.A., Wang, S., Woodbury, N.W. and Allen, J.P. (1992) in: The Photosynthetic Bacterial Reaction Center II: Structure, Spectroscopy, and Dynamics (Breton, J. and Verméglio, A., Eds.), NATO ASI Series A, Vol. 237, pp. 99–108, Plenum Press, New York.
[16] Wachtveitl, J., Farchaus, J.W., Das, R., Lutz, M., Robert, B. and Mattioli, T.A. (1993) Biochemistry 32, 12875–12886.
[17] Deisenhofer, J., Epp, O., Sinning, I. and Michel, H. (1995) J. Mol. Biol. 246, 429–457.
[18] Nabedryk, E., Breton, J., Wachtveitl, J., Gray, K.A. and Oesterhelt, D. (1992) in: The Photosynthetic Bacterial Reaction Center II: Structure, Spectroscopy, and Dynamics (Breton, J. and Verméglio, A., Eds.), NATO ASI Series A, Vol. 237, pp. 147–153, Plenum Press, New York.
[19] Fritzsch, G. (1998) in: Photosynthesis: Molecular Biology of Energy Capture (McIntosh, L., Ed.), Methods in Enzymology, Vol. 297, pp. 57–77, Academic Press, San Diego, CA.
[20] Buchanan, S.K., Fritzsch, G., Ermler, U. and Michel, H. (1993) J. Mol. Biol. 230, 1311–1314.
[21] Otwinowski, Z. and Minor, W. (1997) in: Macromolecular Crystallography (Carter, C.W. and Sweet, R.M., Eds.), Methods in Enzymology, Vol. 276, pp. 307–326, Academic Press, New York.
[22] Brünger, A.T., Adams, P.D., Clore, G.M., DeLano, W.L., Gros, P., Grosse-Kunstleve, R.W., Jiang, J.-S., Kuszewski, J., Nilges, M., Pannu, N.S., Read, R.J., Rice, L.M., Simonson, T. and Warren, G.L. (1998) Acta Crystallogr. D 54, 905–921.
[23] Hodel, A., Kim, S.-H. and Brünger, A.T. (1992) Acta Crystallogr. A 48, 851–858.
[24] Engh, R.A. and Huber, R. (1991) Acta Crystallogr. A 47, 392–400.
[25] Treutlein, H., Schulten, K., Brünger, A.T., Karplus, M., Dei-

senhofer, J. and Michel, H. (1992) Proc. Natl. Acad. Sci. USA 89, 75–79.
[26] Lancaster, C.R.D. and Michel, H. (1997) Structure 5, 1339–1359.
[27] Jones, T.A., Zou, J.-Y., Cowan, S.W. and Kjeldgaard, M. (1991) Acta Crystallogr. A. 47, 110–119.
[28] Evans, S.V. (1993) J. Mol. Graph. 11, 134–138.
[29] Stein, R.R., Castellvi, A.L., Bogacz, J.P. and Wraight, C.A. (1984) J. Cell. Biochem. 24, 243–259.
[30] Leonhard, M. and Mäntele, W. (1993) Biochemistry 32, 4532–4538.
[31] Moss, D., Nabedryk, E., Breton, J. and Mäntele, W. (1990) Eur. J. Biochem. 187, 565–572.
[32] Baymann, F., Moss, D.A. and Mäntele, W. (1991) Anal. Biochem. 199, 269–274.
[33] Bauscher, M., Leonhard, M., Moss, D.A. and Mäntele, W. (1993) Biochim. Biophys. Acta 1183, 59–71.
[34] Leonhard, M. (1992) PhD Thesis, Albert-Ludwigs-Universität Freiburg.
[35] Mäntele, W. (1996) in: Biophysical Techniques in Photosynthesis (Amesz, J. and Hoff, A.J., Eds.), pp. 137–160, Kluwer Academic, Dordrecht.
[36] Brünger, A.T. (1992) Nature 355, 472–475.
[37] Luzzati, V. (1952) Acta Crystallogr. 5, 802–810.
[38] Ramakrishnan, C. and Ramachandran, G.N. (1965) Biophys. J. 5, 909–933.
[39] Abola, E.E., Sussmann, J.L., Prislusky, J. and Manning, N.O. (1997) in: Macromolecular Crystallography (Carter, C.W. and Sweet, R.M., Eds.), Methods in Enzymology, Vol. 277, pp. 556–571, Academic Press, New York.
[40] McAuley-Hecht, K.E., Fyfe, P.K., Ridge, J.P., Prince, S.M., Hunter, C.N., Isaacs, N.W., Cogdell, R.J. and Jones, M.R. (1998) Biochemistry 37, 4740–4750.
[41] Baker, J. (1997) Prog. Biophys. Mol. Biol. 44, 97–179.
[42] Ippolito, J.A., Alexander, R.S. and Christianson, D.W. (1990) J. Mol. Biol. 215, 457–471.
[43] Mattioli, T.A., Williams, J.C., Allen, J.P. and Robert, B. (1994) Biochemistry 33, 1636–1643.
[44] Ivancich, A., Artz, K., Williams, J.C., Allen, J.P. and Mattioli, T.A. (1998) Biochemistry 37, 11812–11820.
[45] Parson, W. and Warshel, A. (1987) J. Am. Chem. Soc. 109, 6152–6163.
[46] Mattioli, T.A., Gray, K.A., Wachtveitl, J., Farchaus, J.W., Lutz, M., Oesterhelt, D. and Robert, B. (1991) in: Spectroscopy of Biological Molecules (Hester, R.E. and Girling, R., Eds.), pp. 71–72, The Royal Society of Chemistry, Cambridge.